Comparison of shallow seismic refraction interpretation methods for regolith mapping

Robert J Whiteley and Peter J Eccleston

Coffey Geotechnics Pty. Ltd.

8/12 Mars Road Lane Cove West

New South Wales, Australia, 2066

Phone: +61 2 9911 1000

Facsimile: +61 2 9911 1001

Email: bob_whiteley@coffey.com.au

Left Running Heading: Whiteley and Eccleston

Right Running Heading: Comparison of refraction methods for regolith mapping

DateStamp: Presented at the 18th ASEG Geophysical Conference & Exhibition (AESC2006), July, 2006. Revised manuscript received 29 September, 2006.

ABSTRACT

A number of shallow refraction interpretation methods are compared in variable regolith conditions using synthetic and published field data. The synthetic model contained a low velocity zone in a depression at the base of the regolith. Independent interpretation with the Reciprocal Method was in reasonable with this model. The Generalised Reciprocal Method performed poorly on this model, both smoothing and considerably underestimating the depth to the simulated regolith base and greatly narrowing the low velocity zone. However, neither the Reciprocal nor Generalised Reciprocal Methods produced valid velocity analyses over the low velocity zone, as diffracted and non-critically refracted wave arrivals are used. Wavefront Eikonal Traveltime Tomography identified the rapid thickening of the regolith over the depression, but introduced an artefact near the low velocity zone, and the regolith base was not easily located. Low wave path densities over the depression identified by this method also indicated that the interpretation should be treated with caution.

The field example was over a variable regolith with a faulted contact between rocks of differing weathering characteristics. Visual Interactive Ray Tracing and Wavefront Eikonal Traveltime Tomographic interpretations were in good general agreement for this example. These interpretations differed considerably from the original Generalised Reciprocal Method interpretation that contained a wide low velocity zone at the contact. This is likely to be an artefact of the Generalised Reciprocal Method interpretation process.

While our comparisons are not definitive and all the interpretation methods that were compared have deficiencies and limitations they do offer some guidance to improving shallow refraction interpretation for regolith mapping. This is achieved by combining some of the methods and involves the Reciprocal Method, Wavepath Eikonal Traveltime Tomography, and Visual Interactive Ray Tracing. Interesting subsurface features and limitations are highlighted by joint use of ray path displays and wave path density diagrams together with various statistical goodness-of-fit measures to the field data. While this interpretation approach should be more robust, it does not eliminate personal bias nor overcome inherent limitations in the shallow seismic refraction method for regolith mapping, such as the delineation of laterally hidden low velocity zones.

Key Words: interpretation, ray tracing, reciprocal, refraction, regolith, seismic, tomography

INTRODUCTION

Shallow seismic refraction is the “work-horse” of engineering geophysics, and has been widely applied to regolith mapping in geotechnical engineering (Whiteley, 1994). Recent interpretation developments have led to this method being increasingly considered as a non-conventional mineral exploration technique for deeper targets within the regolith or near its base. This approach recognises that improved exploration success can only be achieved by having greater understanding of this complex medium (Roach, 2003).

In many prospective areas of Australia, the regolith is highly variable. It can contain both transported sediments and eroded, thick sections of deeply weathered rocks with rapid lateral thickness changes, typically in the range from 0 m to more than 150 m. Theoretically, the base of the regolith should be a continuous seismic refractor, however, depending on lithology and weathering variations it can be a poor seismic refractor at some locations or sufficiently irregular to appear laterally discontinuous from a seismic perspective. Consequently, at a given site, the subsurface seismic velocity distribution within the regolith is rarely known in advance, and it is now usual to acquire redundant, reversed, and overlapping refraction data sets with close geophone and line separations. Typically, geophones are from 2 to 15 m apart with from 5 to 11 sources positioned at 10 to 50 m intervals and extending either side of the linear recording array for distances of 50 to 500 m depending on the subsurface detail desired. Even with this additional field effort it is recognised that not all subsurface refractors will be completely mapped in highly irregular conditions using only first-arrival times.

With the routine acquisition of increased volumes of digital shallow refraction data, the focus of effort is now on the quality and applicability of an increasing range of interpretation approaches and methods. These are still currently 2D but are rapidly evolving to 3D as the sensitivity of the refraction method to regolith variations is being increasingly appreciated. We have chosen to compare some refraction interpretation methods on variable regoliths using synthetic and field data. Our approach is similar to that taken in Europe by Hoffman and Schrott (2003) and Hecht (2003) for regoliths with mainly loose sediments, rather than the deeply weathered regolith that are more common in Australia.

SHALLOW SEISMIC REFRACTION INTERPRETATION

Conventional shallow seismic refraction interpretation methods that are still in common use are based on ray theory (Cerveny and Ravindra, 1971) and derive from either the Delay-time Method (DTM, Barry, 1967; Redpath, 1973) or the Reciprocal (Plus-Minus) Method (RM, Hawkins, 1961; Hagedoorn, 1959). These methods assume that first-arrivals only originate by critical refraction from laterally continuous refractors with relatively simple velocity distributions. They require that arrivals be assigned to individual refractors. In the majority of real situations, the shallow earth is much more complex and these methods become increasingly inaccurate as subsurface variability increases. The RM, incorporating the simpler Intercept-Time method, offers more flexibility in these conditions than the DTM as it assumes locally dipping, rather than horizontal refractor segments. The RM also applies more sophisticated refractor velocity analysis via line-segment fitting to corrected time-depths (i.e., minus-times). With the RM, depth errors caused by lateral velocity variations within the regolith and by incompletely defined shallower refractors are somewhat reduced by linear interpolation of composite velocity terms between source points, where these refractors have been identified. The RM can also be enhanced to evaluate the quality of continuous refractor velocity analyses (e.g., Dampney and Whiteley, 1980) and optimised when shot spacing is sparse in constrained field conditions (e.g., Wright, 2006). An example of a section of deep and variable Western Australia regolith interpreted using the RM (i.e., the plus-minus method) has been provided by Boschetti et al. (1996).

While the RM originated as a manual interpretation method it has evolved to a PC-based method with, for example, REFRACT software (Leung et al. 1997) or its latest version (WINREF, Roads and Traffic Authority, NSW).

The Generalised Reciprocal Method (GRM) was introduced by Palmer (1980) in an attempt to improve the RM by combining laterally migrated first-arrival times. The GRM requires all the model assumptions of the RM with additional assumptions of an “optimum” migration distance (XY) that produces an improved interpretation and can be empirically recovered. Consequently, this method is not strictly a generalisation of the RM but a more restrictive version of the RM. The GRM was also intended to remove “fictitious” higher velocities produced by RM velocity analysis when there are rapid lateral changes in velocity or refractor depth.

The absence of a theoretical and reliable practical basis for selection of “optimum” migration distances has meant that the performance of the GRM in both uniform and variable media being questioned by a number of authors (e.g., Hatherly, 1990; Whiteley, 1990a,b; Sjogren, 2000; Leung, 1995, 2003; Whiteley, 2002). The performance of both the RM and GRM is examined in our comparison.

Like the RM, the GRM originated as a manual method but nowadays can be implemented with commercial software (e.g., IXRefraX, Interpex Ltd.).

Taking an alternative approach, Hatherly (1982) used finite difference methods to numerically solve the 2D seismic wave equation, and demonstrated the importance of diffracted and non-critically refracted waves for shallow refraction interpretation in variable conditions. Hatherly (1982) also showed that ray-based methods were generally applicable in shallow refraction interpretation to practical timing accuracies. Ray-trace modelling software was then produced by Ackermann et al. (1986) for irregular refractors with intervening constant velocity compartments. This automatically accounted for non-critical refraction, and the approach was extended by Leung (1997), who refined the ray-shooting algorithms and added diffractions at compartment boundaries and interfaces. These enhancements provided improved accuracy, flexibility, and stability to ray tracing through highly irregular models with non-continuous refractors and complex velocity distributions. This method was mainly used to check shallow refraction interpretations obtained with the RM, by comparing field data with synthetic data obtained by ray tracing. Sandmeier (2003) has also produced commercial software (REFLEXW) that incorporates network ray tracing, again as a checking tool. Recently, Whiteley (2004) adapted Leung’s (1997) approach to interactive shallow refraction interpretation on a PC screen using Visual Interactive Ray Trace (VIRT) modelling. VIRT is one of the interpretation methods used in this comparison.

As available PC power has increased, other approaches to shallow refraction interpretation have been developed including various forms of refraction tomography (e.g., Zhang and Toksöz, 1998). Sheehan et al. (2005) recently examined some of these methods and compared their performance on a variety of synthetic models with the latest commercial interpretation software. We chose one of these packages, RAYFRACT (Version 2.62, Intelligent Resources Inc.) for our comparison for a variety of reasons, not the least of which was that it does not use a ray approach or require layer assignments to segments of the travel time data. Also, it applies velocity gradients throughout the model in contrast to the discrete constant velocity compartments of the ray-based methods described earlier. RAYFRACT implements Wavepath Eikonal Traveltime Tomography (WET, Schuster and Quintus-Bosz, 1993) with the Fresnel volume approach to inversion developed by Watanabe et al. (1999). This method assumes velocity varies smoothly with depth and allows initial models to be obtained from the Delta-t-v method (Gebrande and Miller, 1985; Rohdewald, in prep.) that is similar to the tau-p method (Barton and Barker, 2003), or from a laterally smoothed version of these models.

We chose to compare the RM, GRM, and WET interpretation methods on synthetic data generated with the VIRT algorithms and GRM, WET, and VIRT interpretations of a published set of shallow refraction field data over a variable regolith.

SYNTHETIC DATA

The 3-layer synthetic model (Model 3L01, from Whiteley, 1990c) in Figure 1 is typical of many similar models that were examined. This contains a 40 m wide low velocity zone below the deeper interface representing a variable regolith base containing a more deeply weathered fault or shear zone. Firstly, the ray-tracing algorithm in the VIRT software was used to generate synthetic first-arrival times at 5 m receiver intervals from multi-offset sources. This data set and first-arrival ray paths from the distant reversed-source pair are also shown in Figure 1.

The synthetic travel-time data, but not the model details, were then provided to an interpreter who independently carried out RM and GRM interpretations. The results obtained are shown in Figure 2 together with the interpreted GRM velocity analysis plot. An "optimum XY" of 10 m was selected by this interpreter for the GRM interpretation according to Palmer's criteria (Palmer, 1980, Ch. 6).

Both the RM and GRM accurately map the upper interface. The deeper interface, representing the base of the regolith, appeared to be defined with reasonable accuracy by the RM but poorly defined by the GRM, particularly in the vicinity of the bedrock depression, where the GRM considerably underestimated depths. On the velocity analysis plot (Figure 2) the GRM at the "optimum XY" of 10 m indicates a narrow low velocity zone about 12 m wide with a velocity of 1500 m/s. The RM has identified a wider low velocity zone, some 26 m wide, extending from about 58 m to 84 m with a velocity of 2300 m/s. This is still somewhat narrower than the actual low velocity zone. The RM has also reported a model violation as an unacceptably high velocity zone on the right side of the low velocity zone. This so-called “fictitious” velocity region is uncertain in the RM interpretation and cannot be used. Such model violations often occur when first arrivals from other than critically refracted waves are combined in the RM and GRM velocity analyses, typically at the sites of abrupt lateral velocity or refractor depth changes. They are not always obvious in RM velocity analysis on synthetic data or on real data, because of measurement errors. Lateral migration of arrivals, applied in the GRM velocity analysis, smooths these features, i.e., essentially ignores this problem.

The ray path diagram (Figure 1) shows that neither the RM nor GRM velocity analyses over the low velocity zone are valid because they are produced using first arrivals from either diffractions or non-critical refractions that originate from the margins of the low velocity zone. Also, as no first-arrival rays have passed through the region in the second layer immediately above the bedrock depression, it is a “laterally hidden zone”. The approximate margins of this zone are defined by the surrounding ray paths, and its maximum velocity is bounded, but its actual velocity is unknown. In a variable regolith such regions occurring in bedrock depressions are relatively common.

Figure 3 shows the WET interpretation of the synthetic data obtained with RAYFRACT software after 300 inversion iterations from a smoothed initial model. The original model is also plotted on Figure 3. As there are actually no vertical velocity gradients within the three layers of this model it is quite difficult for WET inversion. Nevertheless, the WET interpretation has represented significant features of the synthetic model a with region of deepening near the centre of the model being apparent in the velocity contour pattern, but other features of the model are less obvious. The approximate mid-layer velocity in the WET model is close to the specified velocities for the upper layers. The deeper bedrock interface approximately follows the 2400 m/s velocity contour although the true velocities for this layer are not reached until much deeper. However, the left margin of the low velocity zone is not clearly represented on the WET image. The right margin is more distinct but the WET inversion has introduced an artefact in this region of the third layer from about 100 to 120 m. This is the region where the RM velocity analysis also highlighted some problems. The WET interpretation, itself, has provided no information on the laterally hidden zone in the intermediate layer, however the wave path density diagram (Figure 4) that is also an output of the RAYFRACT software shows that the seismic information density is very low within this zone, so again caution is needed in accepting the WET interpretation. This is a very useful display, akin to the ray path diagram in VIRT, which calls attention to significant parts of the model including, in this case, the laterally hidden zone in the intermediate layer.

FIELD DATA

A set of refraction field data over a variable regolith has been provided by Palmer (1980, Line 4, p.99–101). This was acquired with a 10 m geophone and 60 m source interval. A 4-layer, GRM interpretation was also presented (Palmer, 1980, Fig. 51) and is shown in

Figure 6. This interpretation has identified a wide low velocity zone within the deepest refractor, possibly representing a fault and a substantial change in regolith thickness across this structure. This is represented mainly by the thickening of the third layer that was assigned a uniform velocity of 1600 m/s in the GRM interpretation.

VIRT was independently applied to this data set and also produced a 4-layer interpretation that reasonably fits field data over the structure. The VIRT interpretation, field and computed travel-time data with first arrival ray paths from the end source points are shown in Figure 5. This interpretation also shows the substantial change in regolith thickness that was identified in the GRM interpretation. However, no low velocity zone was identified in the VIRT interpretation at the structure near Ch. 1170 m, and there was a substantial lateral change in the velocity of the third layer from 2600 m/s to 1800–2000 m/s across the structure and in the fourth layer from 4700 m/s to 3100–3400 m/s. The first-arrival ray paths from the deepest refractor near the centre of the profile show that non-critical refractions with penetration into this layer, and diffractions from lateral velocity changes, are major contributors to the first arrivals over the structure. As noted earlier these paths are not considered in either RM or GRM interpretation processes.

The GRM and VIRT interpretations are compared in Figure 6. Both show a large lateral velocity change across the contact within the fourth layer representing the base of the regolith, but there are significant differences in velocity distribution in the upper layers and in the depth to the second and third interface, particularly, on the left side of the section.

The WET model obtained after 20 iterations using a smoothed-gradient initial model is shown in Figure 7, with the corresponding wave path density diagram. This model closely fitted the field data with a maximum unsigned error of 2.2 ms. It shows an abrupt depth change across the structure with very different velocity gradients on either side, consistent with different lithologies and weathering characteristics. Again, no low velocity zone is indicated in the WET interpretation at the structure. The wave path density diagram in Figure 7 shows a concentration within the higher velocity shallower bedrock to the left and a reduction in the deeper regions immediately to the right of the structure. This effect was noted in the synthetic model (Fig.4) when a rapid refractor deepening occurred.

Finally, the VIRT and WET interpretations are compared in Figure 8. These interpretations indicate a thicker lower velocity regolith on the right side of the structure. This suggests a gradual decrease in weathering with depth is more appropriate for the deeply weathered rocks on the right side of the model below about 50 m depth.

CONCLUSIONS

For the synthetic example, representing a low velocity zone at the base of the regolith, the RM appeared to provide a reasonable interpretation. RM velocity analysis highlighted areas of model violation but did not identify the causes of the problem. These are related to the use, in RM and GRM interpretations, of unrecognised diffracted and non-critically refracted arrivals that occur over abrupt structures. These events invalidate velocity analyses obtained with both the RM and GRM over the thicker regolith section. The GRM performed poorly for this model, both smoothing and underestimating depths to the deepest interface in the depression and greatly narrowing the low velocity zone.

WET inversion allowed a major feature of the synthetic model, i.e., the rapid thickening of the regolith, to be observed, but an artefact was introduced near rapid lateral velocity changes. The WET wave path density diagram for this model showed low densities over the major feature which indicated that this interpretation should also be treated with caution. The WET interpretation also did not accurately locate the interfaces where large and abrupt velocity contrasts were present.

For the field example over a variable regolith, the VIRT and WET interpretations were in good general agreement and located an abrupt structure probably representing a faulted contact with rock of differing weathering characteristics on either side. These methods do not agree with the GRM interpretation nor do they substantiate a wide low velocity zone at the contact. This is likely to be an artefact of the GRM interpretation. Further, the GRM interpretation applied a heavily smoothed or single averaged overburden velocity distribution that is clearly inappropriate for this data set.

While our comparisons are not definitive and all of the interpretation methods we compared have deficiencies and limitations they do offer some guidance for more robust approaches to shallow refraction interpretation for regolith mapping. Our currently preferred approach is summarised in Table 1.

Firstly, this involves applying the RM that incorporates editing and parallelism testing of redundant, single direction first-arrival data sets. This allows overall data characteristics, quality and limitations to be quickly assessed and provides first-pass interpretations. The velocity analysis process in the RM highlights possible low velocity zones and model violations where fictitious high velocities are observed. WET can also be applied to the edited data set to generate first-pass interpretations, and for further modelling using a range of starting models. These can be guided by the first-pass interpretation and include any independent information if desired, but this is not necessary. As inversion methods are progressing rapidly it is also relatively easy to incorporate these at this interpretation stage. VIRT can be applied at any time in the process to develop initial models for survey design, to check and modify RM or WET models, and to further highlight model deficiencies and limitations. This is achieved by joint use of ray path displays and wave path density diagrams together with various statistical goodness-of-fit measures to the field data. The overall process provides the interpreter with considerable opportunity to interact with the models and data but does not, of course, eliminate personal bias or the deficiencies of the individual refraction interpretation methods. However, the WET and VIRT methods do provide models that agree with the field data. This cannot be assured with the RM and GRM methods. As a further cautionary note, even this more powerful combination of shallow refraction interpretation tools does not overcome the inherent limitations in the shallow seismic refraction method for regolith mapping, such as the presence of laterally hidden low velocity zones.

ACKNOWLEDGEMENTS

Maung Aung Win interpreted the synthetic model data in Figure 1 and Tak Ming Leung developed the ray trace model in Figure 5.

REFERENCES

Ackermann H.D., Pankratz, L.W., and Dansereau, D., 1986, Resolution of ambiguities of shallow refraction travel-time curves: *Geophysics*, **51**, 223–235.

Barry, K.M., 1967, Delay-time and its application to refraction profile interpretation: in Musgrave, A.W. (ed.), *Seismic Refraction Prospecting*: Society of Exploration Geophysicists, 348–361.

Barton, R., and Barker, N., 2003, Velocity imaging by tau-p transformation of refracted traveltimes: *Geophysical Prospecting*, **51**, 195–203.

Boschetti, F., Dentith, M.C., and List, R.D., 1996, Inversion of seismic refraction data using genetic algorithms: *Geophysics*, **61**, 1715–1727.

Cerveny, V., and Ravindra, R., 1971, *Theory of Seismic Head Waves*: Toronto Press, 296p.

Dampney, C.N.G., and Whiteley, R.J., 1980, Velocity determination and error analysis for the shallow seismic refraction method: *Geophysical Prospecting*, **18**, 2–17.

Gebrande, H., and Miller, H., 1985, Refractionsseismik, in Bender, F., (ed.), *Angewandte Geowissenschafen II*: Ferdinand Enke, 226–260.

Hagedoorn, J.G., 1959, The plus-minus method of interpreting seismic refraction sections: *Geophysical Prospecting*, **7**, 158–182.

Hatherly, P.J., 1982, Wave equation modelling for the shallow seismic refraction method: *Exploration Geophysics*, **13**, 27–34.

Hatherly, P.J., 1990, Comments on Engineering Geophysics – A Geophysicist's View by R.J. Whiteley: *Exploration Geophysics*, **21**, 139–142.

Hawkins, L.V., 1961, The Reciprocal method of routine shallow seismic refraction investigations: *Geophysics*, **26**, 806–819.

Hecht, S., 2003, Differentiation of loose sediments with seismic refraction methods – potentials and limitations derived from case studies: in Schott, L., Hordt, A., and Dikau, R. (eds), *Geophysical Applications in Geomorphology*: Annals of Geomorphology, Supp. Vol. 132, Gebruder Borntraeger, 89–102.

Hofmann, T., and Schrott, L., 2003, Determining sediment thickness of talus slopes and valley fill deposits using seismic refraction – a comparison of 2D interpretation tools: in Schott, L., Hordt, A., and Dikau, R. (eds), *Geophysical Applications in Geomorphology*: Annals of Geomorphology, Supp. Vol. 132, Gebruder Borntraeger, 71–87.

Leung T.M., 1995, Examination of the optimum XY value by ray tracing: *Geophysics*, **40**, 1151–1156.

Leung, T.M., Win, A.W., Walker, C.S., and Whiteley, R.J., 1997, A flexible algorithm for seismic refraction interpretation using program REFRACT: in McCann, D.M., Eddleston, D.M., Fenning, P.J., and Reeves, G.M. (eds), *Modern Geophysics in Engineering Geology*: Geological Society of London, Engineering Geology Special Publication No. 12, 399–407.

Leung, T.M., 1997, Evaluation of seismic refraction using first arrival raytracing: in McCann, D.M., Eddleston, D.M., Fenning, P.J., and Reeves, G.M. (eds), *Modern Geophysics in Engineering Geology*: Geological Society of London, Engineering Geology Special Publication No. 12, 413–416.

Leung, T.M., 2003, Controls of traveltime data and problems with the generalized reciprocal method: *Geophysics*, **68**, 1626–1632.

Palmer, D., 1980, *The generalized reciprocal method of seismic refraction interpretation*: Society of Exploration Geophysics, 104p.

Redpath, B., 1973, *Seismic refraction for engineering site investigation*: Explosives Excavation Research Lab., TR E-73-4, 51p.

Roach, I.C., (ed.), 2003, Advances in Regolith: *Proceedings of the CRC LEME Regional Regolith Symposia*, 2003.

Rohdewald, S.R., (in prep.), Delta-t-v 1D seismic refraction inversion method: theory.

Sheehan, J.R., Doll, W.E., and Mandell, W.A., 2005, An evaluation of methods and available software for seismic refraction tomography analysis: *Journal of Environmental and Engineering Geophysics*, **10**, 21–34.

Sandmeier, K.J., 2003, Refraction seismic demo REFLEXW V.3.0: Supp. CD in Schott, L., Hordt, A., and Dikau, R. (eds), *Geophysical Applications in Geomorphology*: Annals of Geomorphology, Supp. Vol. 132, Gebruder Borntraeger.

Schuster, G.T., and Quintus-Bosz, A., 1993, Wavepath eikonal traveltime inversion: *Geophysics*, **58**, 1314–1323.

Sjogren, B., 2000, A brief study of the generalized reciprocal method and some limitations of the method: *Geophysical Prospecting*, **48**, 815–834.

Walker, C., Leung, T.M., Win, M.A., and Whiteley, R.J., 1991, Engineering seismic refraction: an improved field practice and a new interpretation method: *Exploration Geophysics*, **22**, 423–426.

Watanabe, T., Matsuoka, T., and Ashida, Y., 1999, Seismic traveltime tomography using Fresnel volume approach: *69th Annual International Meeting of the Society of Exploration Geophysicists, Expanded Abstracts*, SPRO12.5.

Whiteley, R.J., 1990a, Engineering geophysics - a geophysicist's view: *Exploration Geophysics*, **21**, 7–16.

Whiteley, R.J., 1990b, Discussion: *Exploration Geophysics*, **21**, 131–138.

Whiteley, R.J., 1990c, Advances in engineering seismics: Keynote address, Remote Sensing and Geophysical Techniques, Theme 2, *Proceedings of the 6th IAEG Congress,* **2**, 813–825.

Whiteley, R.J., 1994, Seismic refraction testing - a tutorial: in Richard D. Woods, R.D. (ed.), *Geophysical Characterization of Sites*: Oxford & IBH Publishing, 45–47.

Whiteley, R.J., 2002, Shallow refraction interpretation in complex conditions with visual interactive ray tracing: *64th EAGE Conference & Exhibition*, paper P155.

Whiteley, R.J., 2004, Shallow seismic refraction interpretation with visual interactive raytracing (VIRT): *Exploration Geophysics,* **35**, 116–123.

Wright, C., 2006, The LSDARC method of refraction analysis: principles, practical considerations and advantages: *Near Surface Geophysics,* **4**, 189–202.

Zhang, J., and Toksöz, M.N., 1998, Nonlinear refraction traveltime tomography: *Geophysics*, **63**, 1726–1737.

TABLE

Table 1:

Shallow Refraction Interpretation System for Detailed Regolith Mapping

Interpretation Method	Application
VIRT	Refraction survey design
RM	T-X data edits
RM/WET	First-pass interpretations
WET	Inversions with various initial models
VIRT	Model testing and refinement

FIGURE CAPTIONS

Fig. 1:

Synthetic Model 3L01 with *t-x* plots and first arrival ray paths from distant sources.

Fig. 2:

RM and GRM interpreted models with velocity analyses.

Fig. 3:

WET interpretation and original synthetic model.

Fig. 4:

Wavepath density diagram for the synthetic WET model.

Fig. 5:

VIRT interpreted model and field data over a variable regolith.

Fig. 6:

(a) GRM interpretation, after Palmer (1980), and (b) VIRT interpretation.

Fig. 7:

WET interpreted model and wavepath density diagram.

Fig. 8:

Comparison of VIRT and WET interpretations.

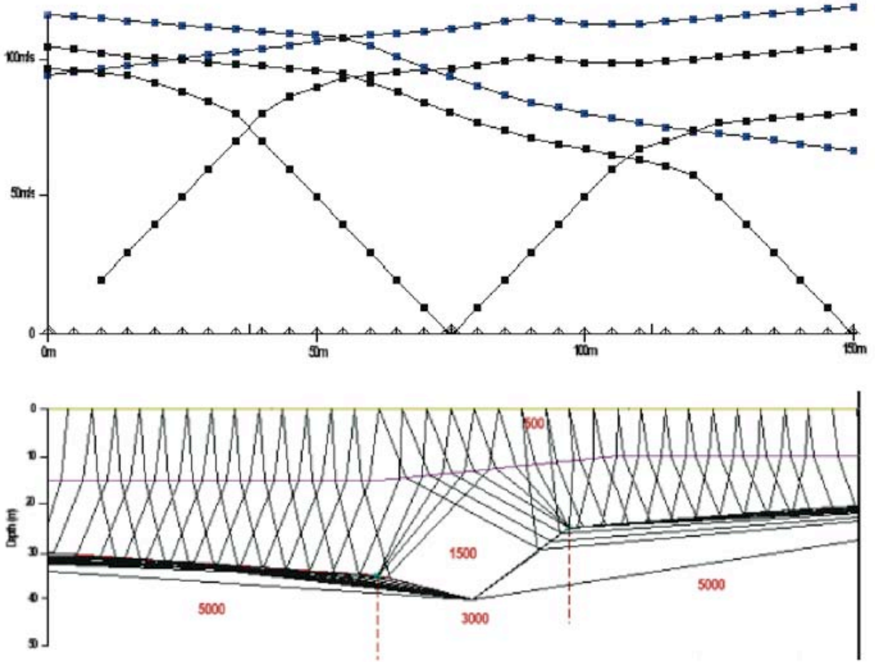
0
0m
50m
100m
150m
0
10
20
30
40
50
Depth (m)
500
1500
5000
3000
5000

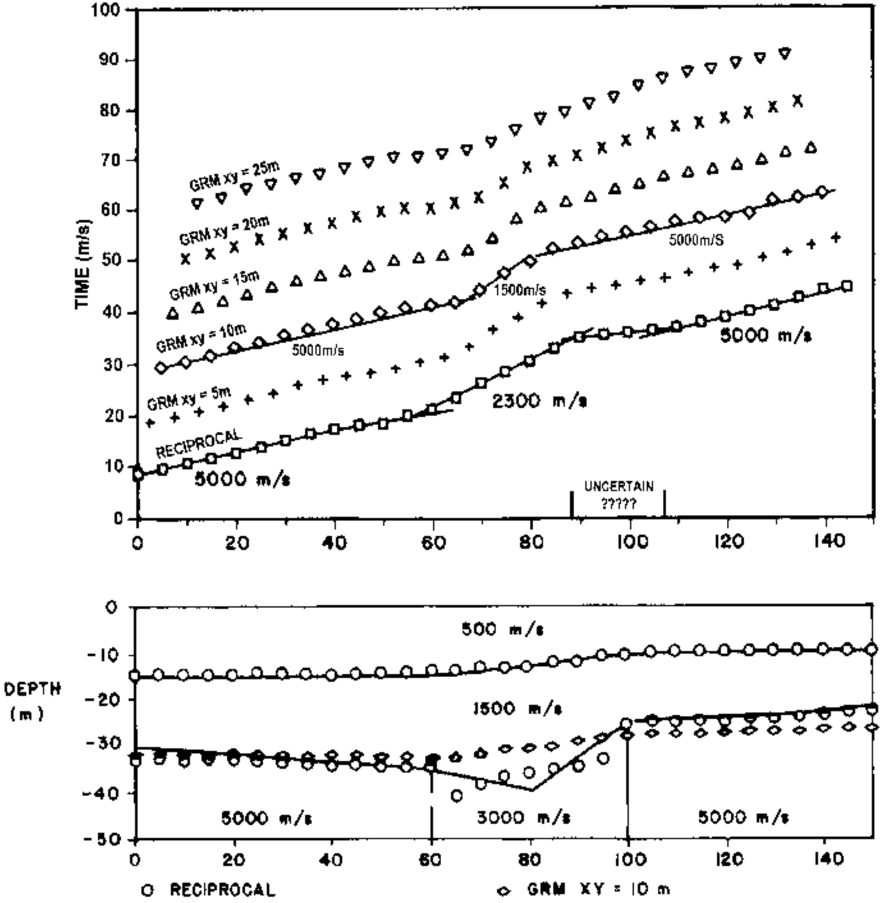

TIME (m/s)
GRM xy = 25m
GRM xy = 20m
GRM xy = 15m
GRM xy = 10m
GRM xy = 5m
RECIPROCAL
5000m/s
1500m/s
5000m/S
5000 m/s
2300 m/s
5000 m/s
UNCERTAIN
?????
DEPTH (m)
500 m/s
1500 m/s
5000 m/s
3000 m/s
5000 m/s
RECIPROCAL
GRM XY = 10 m

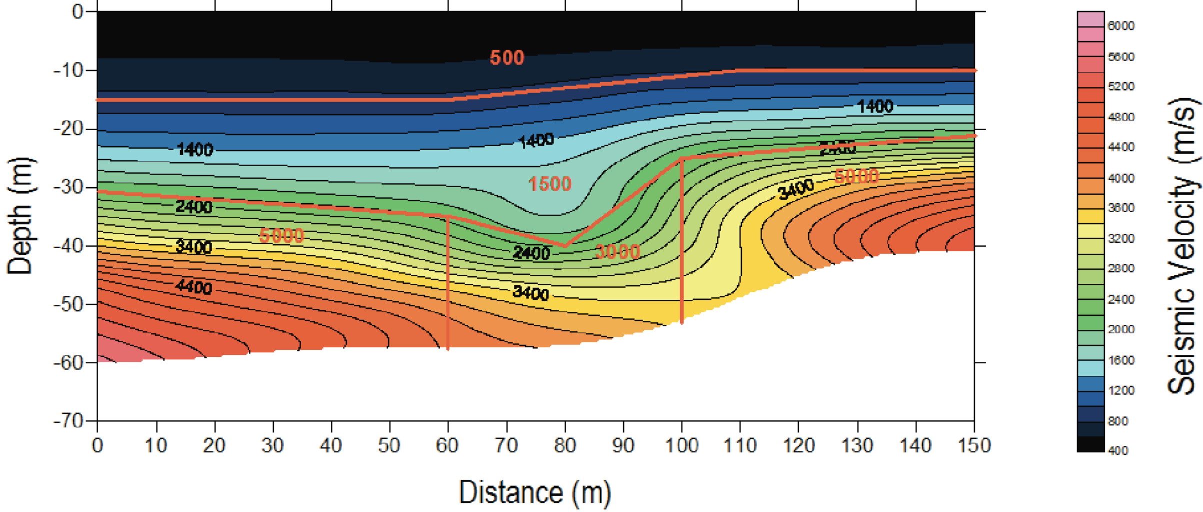

Depth (m)
Distance (m)
Seismic Velocity (m/s)
500
1400
1400
1400
1500
2400
2400
3400
3400
3400
4400
5000
5000
3000
0
-10
-20
-30
-40
-50
-60
-70
0
10
20
30
40
50
60
70
80
90
100
110
120
130
140
150
6000
5600
5200
4800
4400
4000
3600
3200
2800
2400
2000
1600
1200
800
400

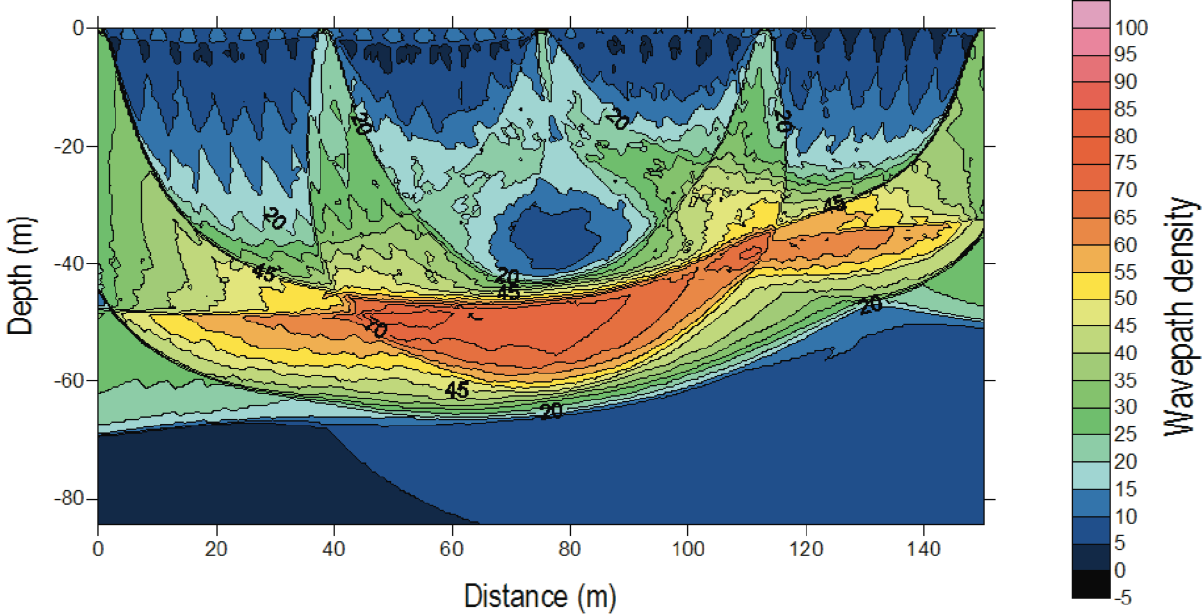

0
-20
-40
-60
-80
Depth (m)
0
20
40
60
80
100
120
140
Distance (m)
20
20
20
20
20
20
20
20
45
45
45
45
70
100
95
90
85
80
75
70
65
60
55
50
45
40
35
30
25
20
15
10
5
0
-5
Wavepath density

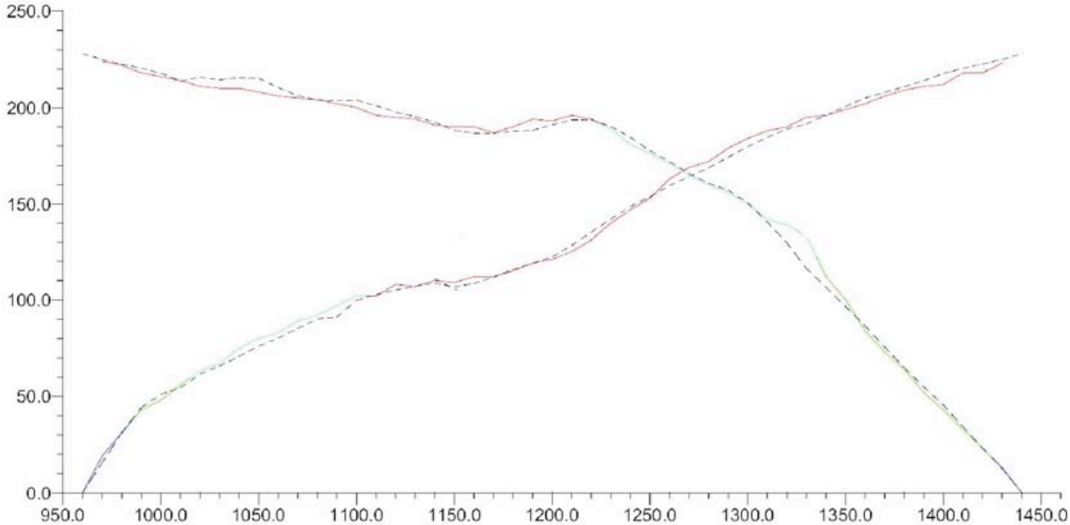
250.0
200.0
150.0
100.0
50.0
0.0
950.0
1000.0
1050.0
1100.0
1150.0
1200.0
1250.0
1300.0
1350.0
1400.0
1450.0

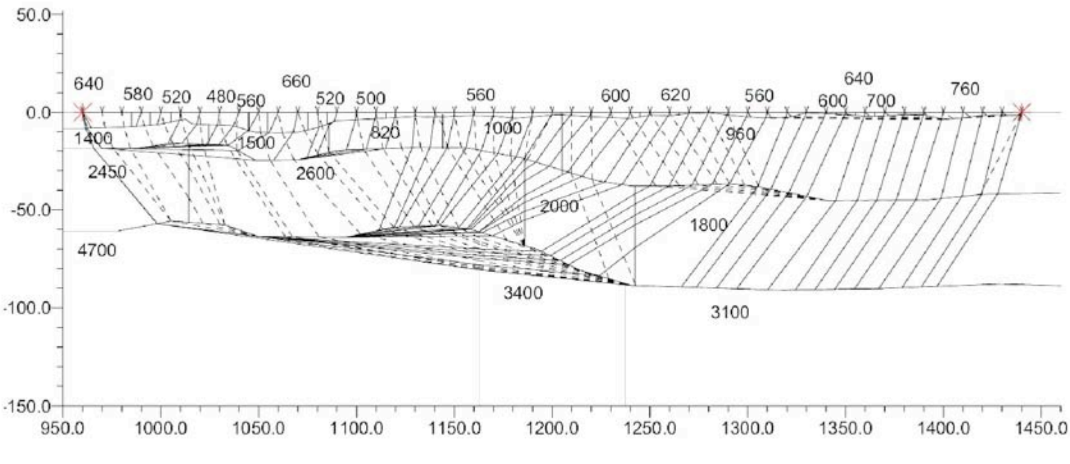
50.0
0.0
-50.0
-100.0
-150.0
950.0
1000.0
1050.0
1100.0
1150.0
1200.0
1250.0
1300.0
1350.0
1400.0
1450.0
640
580
520
480
560
660
520
500
560
600
620
560
640
600
700
760
1400
1500
820
1000
960
2450
2600
2000
1800
4700
3400
3100

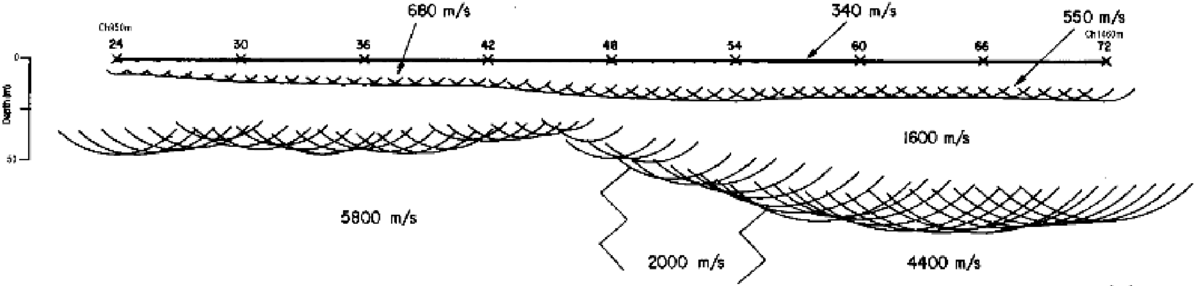
680 m/s
340 m/s
550 m/s
24
30
36
42
48
54
60
66
72
1600 m/s
5800 m/s
2000 m/s
4400 m/s

(a)

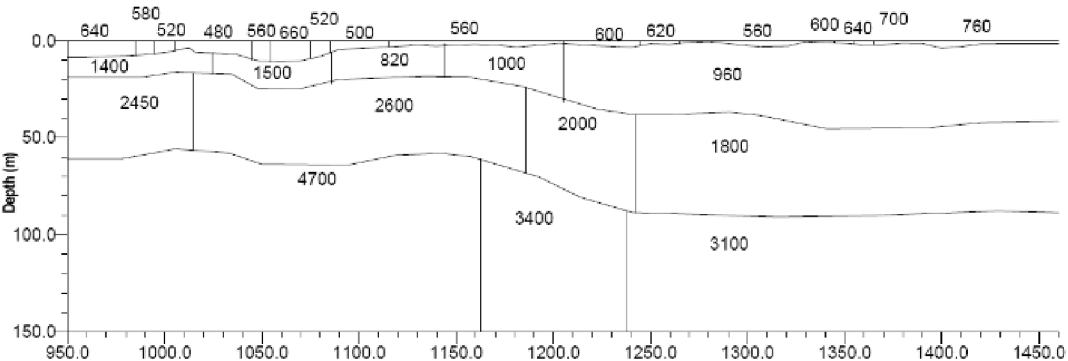
640
580
520
480
560
660
520
500
560
600
620
560
600
640
700
760
1400
1500
820
1000
960
2450
2600
2000
1800
4700
3400
3100
Depth (m)
0.0
50.0
100.0
150.0
950.0
1000.0
1050.0
1100.0
1150.0
1200.0
1250.0
1300.0
1350.0
1400.0
1450.0

(b)

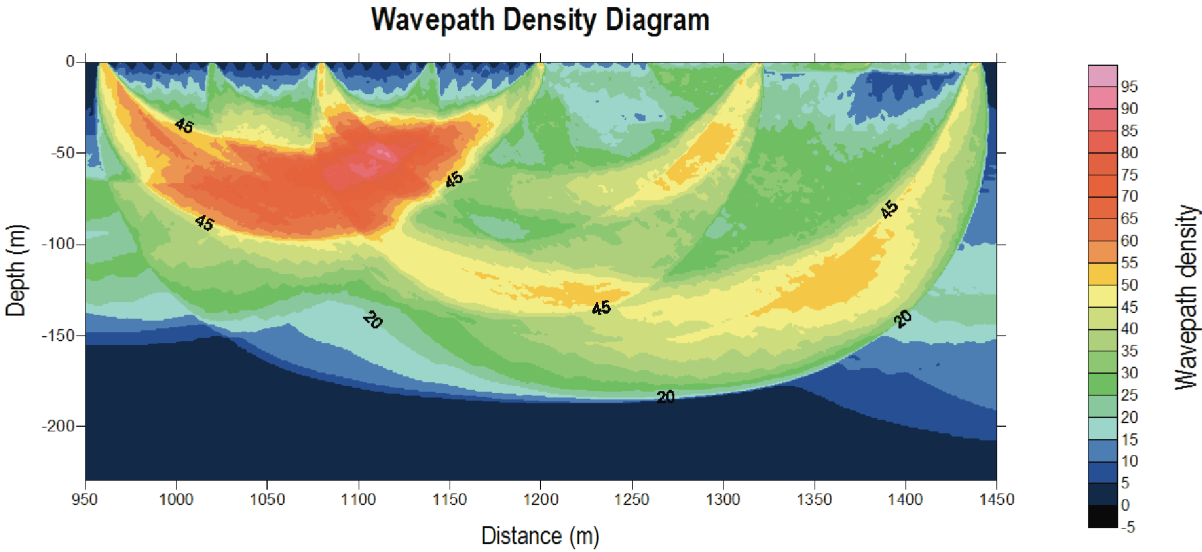
Wavepath Density Diagram
Depth (m)
Distance (m)
Wavepath density
0
-50
-100
-150
-200
950
1000
1050
1100
1150
1200
1250
1300
1350
1400
1450
45
20
95
90
85
80
75
70
65
60
55
50
45
40
35
30
25
20
15
10
5
0
-5

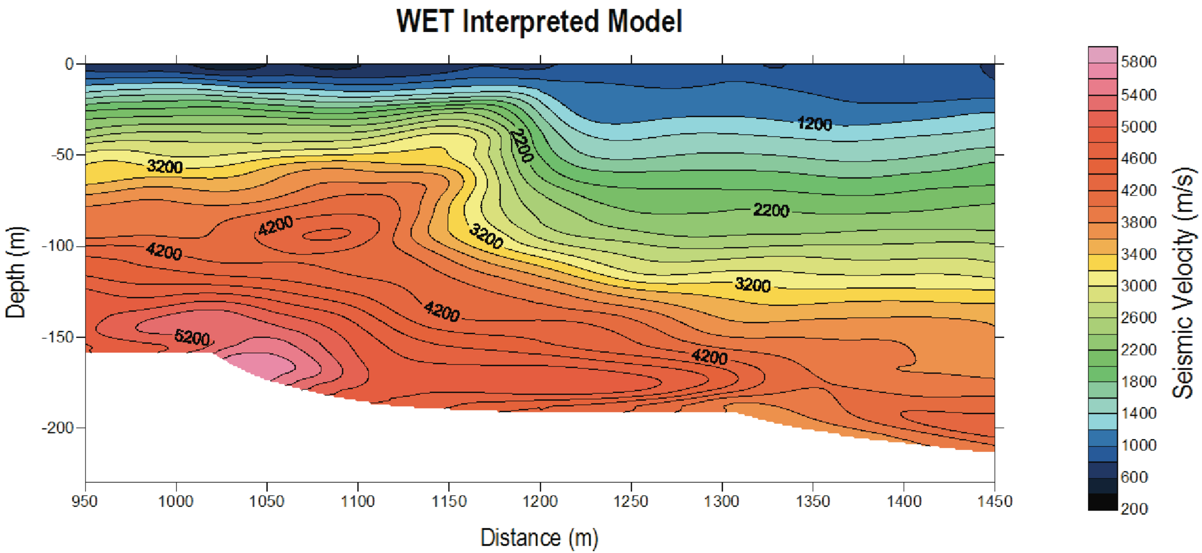
WET Interpreted Model
Depth (m)
Distance (m)
Seismic Velocity (m/s)
0
-50
-100
-150
-200
950
1000
1050
1100
1150
1200
1250
1300
1350
1400
1450
1200
2200
3200
4200
5200
5800
5400
5000
4600
4200
3800
3400
3000
2600
2200
1800
1400
1000
600
200

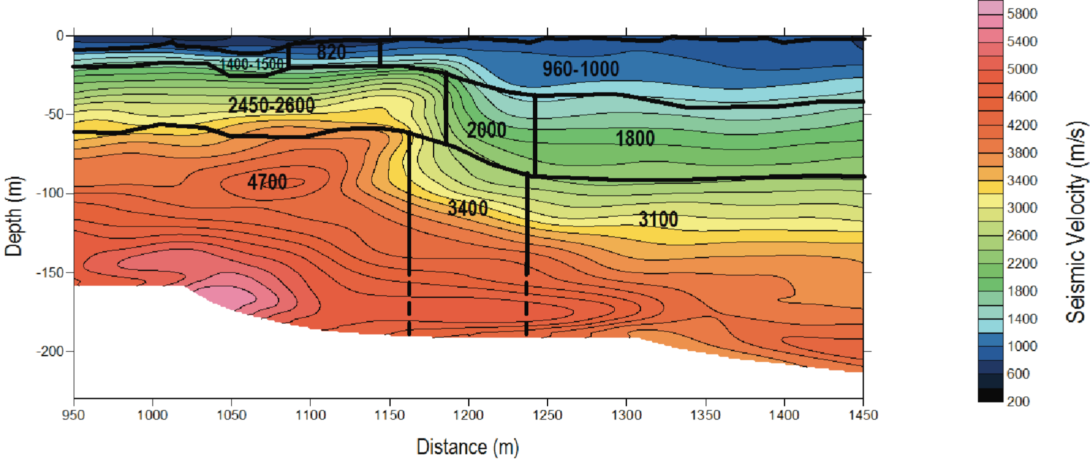

0
-50
-100
-150
-200
Depth (m)
820
1400-1500
960-1000
2450-2600
2000
1800
4700
3400
3100
950
1000
1050
1100
1150
1200
1250
1300
1350
1400
1450
Distance (m)
5800
5400
5000
4600
4200
3800
3400
3000
2600
2200
1800
1400
1000
600
200
Seismic Velocity (m/s)